Elastic, quasielastic, and inelastic neutron-scattering studies on the charge-transfer hexamethylbenzene-tetracyanoquinodimethane complex

Wanda Sawka-Dobrowolska, Grażyna Bator, and Lucjan Sobczyk[a)]
Faculty of Chemistry, University of Wrocław, 50-383 Wrocław, Joliot-Curie 14, Poland

Andrzej Pawlukojć and Halina Ptasiewicz-Bak
Institute of Nuclear Chemistry and Technology, 03-195 Warszawa, Dorodna 16, Poland and Joint Institute for Nuclear Research, 141980 Dubna, Russia

Håkan Rundlöf
Neutronforskningslaboratoriet (NFL) Studsvik, S-61182 Nyköping, Sweden

Jan Krawczyk, Małgorzata Nowina-Konopka, Piotr Jagielski, and Jerzy A. Janik
H. Niewodniczański Institute of Nuclear Physics PAN, 31-342 Kraków, Poland

Michael Prager
Institut für Festkörperforschung, Forschungszentrum Jülich, D-52425 Jülich, Germany

Olav Steinsvoll
Institute for Energy Technology, 2007 Kjeller, Norway

Eugeniusz Grech and Joanna Nowicka-Scheibe
Institute of Chemistry and Environmental Protection, Szczecin University of Technology, 71-065 Szczecin, Al. Piastów 12, Poland

(Received 11 May 2005; accepted 22 June 2005; published online 27 September 2005)

The 1:1 hexamethylbenzene (HMB)-tetracyanoquinodimethane (TCNQ) complex shows a first-order phase transition at 230/218 K (heating/cooling) with no change of the space group. The neutron-diffraction studies reveal that this transition is related to a freezing of the rotation of methyl groups. The results for 100 K enabled precise determination of configuration of HMB·TCNQ complexes. The planes of HMB and TCNQ molecules from small angle (6°) so that the dicyanomethylene group approaches the HMB molecule to a distance of 3.34 Å. The conformation of methyl groups was exactly determined. The quasielastic neutron-scattering spectra can be interpreted in terms of 120° jumps with different activation barrier in low- and high-temperature phases, equal to 3.7 and 1.8 kJ/mol, respectively. These values are lower than that for neat HMB (6 kJ/mol). The conclusion can be drawn that the methyl groups can reorient more freely in the complex. This conclusion is in agreement with the results of inelastic neutron-scattering studies of low-frequency modes assigned to torsional vibrations of methyl groups. These frequencies are lower than those for neat HMB. The analyzed increase of frequencies of these modes as compared with free molecules can be interpreted as due to formation of unconventional C–H···Y hydrogen bonds which are more pronounced in crystals of neat HMB than in those of HMB·TCNQ. The low-frequency librational modes can be treated as a sensitive measure of unconventional hydrogen bonds formed by the CH_3 groups. © *2005 American Institute of Physics*. [DOI: 10.1063/1.2035077]

I. INTRODUCTION

Hexamethylbenzene (HMB) belongs to interesting compounds due to its high symmetry of a flapjack form and unusual dynamics resulting from the fast reorientation of methyl groups in the solid state and perhaps the rotation around the sixfold symmetry axis. In the recently published paper[1] HMB is compared with a chemical conundrum in the sense that at room temperature and on the short time scale an almost infinite number of possible conformations related to the arrangement of hydrogen atoms does exist. The unusual dynamics leads to two phase transitions in the solid state interpreted as due to restrains of rotations of either the whole molecules or methyl groups. The phase transitions were reported in several papers:[2] at 115–118 K ($\Delta H = 1.1$ kJ mol^{-1}, $\Delta S = 9-10$ J mol^{-1} K^{-1}) and at 384 K ($\Delta H = 1.5-1.8$ kJ mol^{-1}, $\Delta S \approx 5$ J mol^{-1} K^{-1}).

The structure of HMB was the subject of several studies by using both the x-ray and neutron-diffraction techniques.[1,3–6] Unfortunately, the dominating opinion is that until now the structure of HMB molecules was not completely solved in all three solid phases. However, there are no doubts that difficulties arise from the unusual dynamics. The role of that dynamics was the subject of a number of NMR studies, and particularly on fully deuterated HMB-d_{18}.[7–12] Recently performed quasielastic neutron-scattering (QENS)

[a)]Author to whom correspondence should be addressed: Electronic mail: sobczyk@wchuwr.chem.uni.wroc.pl

and inelastic neutron-scattering (INS) studies[13] are consistent with the complex picture of dynamics of HMB crystals.

The subject of our interest in this paper is the complex of HMB with tetracyanoquinodimethane (TCNQ). We have been interested in the dynamics of HMB molecules subjected to charge-transfer (CT) interactions with rather strong electron-acceptor counterpart. In other words, the problem is how the HMB molecule will behave in a matrix formed by the electron-accepting molecules. HMB with markedly manifested electron-donor properties was studied in many papers as a component of the CT complexes. The overview of CCDC base shows that the structures of the following HMB complexes were investigated: with chloranil,[14] tetracyanoethylene (TCNE),[15] 1,3,5-trichloro-2,4,6-tricyanobenzene,[16] hexafluorobenzene,[17] bromanil,[18] 1,3,5-tricyanobenzene,[19] and fluranil.[20] A general analysis of the charge-transfer effects in the π complexes from the point of view of the structure was published by Le Magueres *et al.*[21]

The HMB·TCNQ complex was already studied by the x-ray diffraction.[22,23] It was shown that the structure consists of infinite sheets of HMB molecules alternately stacked with sheets of TCNQ molecules approximately parallel to the $10\bar{1}$ plane. From another viewpoint there are infinite columns of alternate HMB and TCNQ molecules parallel to the *a* axis. A rotational disorder of HMB molecules was pointed out.

The aim of our studies was first of all to determine the structure of HMB·TCNQ complex at room and low temperature by using neutron-diffraction technique and look for a possible phase transitions related to the freezing of HMB molecule motions. Another important aspect of our studies is the problem of the rotational potential of methyl groups affected by intermolecular interactions. This is seen in tunnel splitting and low-frequency torsional vibrations which are well reflected in the INS spectra. In many cases this technique appeared to be a unique method enabling insight to the dynamics of methyl groups. These problems were discussed in several review articles.[24–28] We want to compare the INS low-frequency spectra for HMB with its complex followed by a theoretical analysis based on the density-functional theory (DFT) calculations. An important task of our investigations was also to study the QENS spectra over a broad temperature range, which allows one to conclude about the dynamics of methyl groups and particularly about the barrier height of rotation.

II. METHODOLOGY

A. Experimental methods

Large crystals of HMB·TCNQ ($\sim$0.5 cm^3) were grown from CH_3CN solution by a slow evaporation of the solvent at room temperature.

The X-ray diffraction data (I) were measured at 100 K on a KUMA KM4 charge-coupled device (CCD) four-circle diffractometer with graphite monochromated Mo K_α radiation. The space group $I2/m$ was chosen from systematic absences and subsequent least-squares refinement.

The structure was solved by direct methods [SHELXS97 (Ref. 29)] and refined by full-matrix least squares on F^2 using SHELXL97 (Ref. 30) programs. Nonhydrogen atoms were refined with anisotropic thermal parameters. All positions of the H atoms were found from difference Fourier maps and refined isotropically. During the refinement an extinction correction was applied without any absorption correction.

The neutron-diffraction data were collected at 295 and 100 K at the R2 reactor in Studsvik, Sweden, in a beam of wavelength of 1.2055 Å obtained by reflection from a Cu(220) double monochromator. The four-circle diffractometer was equipped with a two-stage closed-cycle helium refrigerator. All reflections were measured in the $\theta-2\theta$ mode, step scan with $\Delta\theta=0.10^\circ$, 40 steps, and minimum time 10 s per step.

The unit-cell dimensions were determined from single-crystal x-ray study. Cell dimensions determined from single-crystal neutron-diffraction data, 16 reflections in the 2θ interval $40^\circ-60^\circ$, are not significantly different, but as the precision in the x-ray cell dimensions is significantly better, the x-ray results have been used in the present neutron investigation. Background correction following Lehmann Larsen[31] and Lorentz correction were applied. Absorption correction by Gaussion integration[32] and extinction correction were done.

The scattering lengths for N, C, and H were 0.0936, 0.06646, and -0.3739×10^{-12} cm, respectively, taken from Sears.[33]

The relative coordinates of heavy atoms and hydrogen atoms were used as starting model from the low-temperature x-ray measurement.

Full-matrix least-squares refinement was done with the program UPALS (Ref. 34) and completed using SHELXL97.[30]

In the case of sample II the hydrogen atoms of two methyl groups were found to be disordered: in each case the disorder was modeled using two set of sites: for the H4, H5, and H6 hydrogen atoms connected to C14 the refined values of the site-occupancy factors were 0.6/0.4, 0.6/0.4, and 0.7/0.3, respectively, while for H2 bonded to C13 it was 0.6/0.4. The occupancy factors were fixed during the final refinement.

For sample III in the final stages of refinement, positional, and anisotropic atomic displacement parameters were refined for all H atoms. The data collection parameters for x-ray and neutron-diffraction methods are summarized in Table I.

The QENS spectra were measured with the time-or-flight spectrometer (TOF), operating at the JEEP II reactor at the Institute of Energy Technology, Kjeller, Norway. Neutrons coming from a cold neutron source were monochromatized to the energy of 4.66 meV by a Bragg scattering from a pyrolytic graphite crystal. The QENS spectrum measurements were performed for one scattering angle 80°, corresponding to the momentum transfer of 1.9 $Å^{-1}$ at temperatures from 10 K up to room temperature. The energy resolution of the TOF spectrometer was ca. 0.25-meV full width at half maximum (FWHM).

The powder sample was contained in a flat aluminum sample holder of the size of about $40\times50\times1$ mm^3. The obtained spectra were corrected for the sample-holder scattering. Multiple scattering corrections were applied as well. The instrumental resolution function was determined by

TABLE I. Crystal data and structure refinement.

Crystal data	I	II	III
Empirical formula	$C_{12}H_{18}\cdot C_{12}H_4N_4$	$C_{12}H_{18}\cdot C_{12}H_4N_4$	$C_{12}H_{18}\cdot C_{12}H_4N_4$
Formula weight ($g\,mol^{-1}$)	366.23	366.23	366.23
Crystal system	Monoclinic	Monoclinic	Monoclinic
Space group	$12/m$	$12/m$	$12/m$
a (Å)	8.234(2)	8.305(2)	8.234(2)
b (Å)	13.440(2)	13.547(2)	13.440(2)
c (Å)	8.997(3)	9.193(3)	8.997(3)
β (°)	92.26(3)	94.01(3)	92.26(32)
V ($Å^3$)	994.9(4)	1032.3(4)	994.9(4)
Z	2	2	2
D_{calc} ($g\,cm^{-3}$)	1.223	1.186	1.223
μ (mm^{-1})	0.074	0.184	0.184
Crystal size (mm)	$0.30\times0.3\times0.33$	$1.1\times1.6\times1.9$	$1.1\times1.6\times1.9$
Data collection			
Diffractometer	KM4CCD	Huber-Aracor 400-mm diameter four-circle	Huber-Aracor 400-mm diameter four-circle
Data collection method	ω	$\theta-2\theta$ scans	$\theta-2\theta$ scans
Radiation type	Mo K_α	Neutron	Neutron
Wavelength (Å)	0.7073	1.2055	1.2055
T (K)	100(2)	295(2)	100(2)
θ_{max} (°)	28.5	52	52
Indexes range	$-11\leqslant h\leqslant 6$	$0\leqslant h\leqslant 10$	$-2\leqslant h\leqslant 10$
	$-17\leqslant k\leqslant 17$	$0\leqslant k\leqslant 17$	$-8\leqslant k\leqslant 17$
	$-11\leqslant l\leqslant 12$	$-12\leqslant l\leqslant 11$	$-11\leqslant l\leqslant 11$
Absorption correction	None	Numerical	Numerical
min, max absorption correction		0.6140, 0.7206	0.6139, 0.7205
No. of measured, independent parameters	3466, 1195	1336, 1255	1424, 1206
R_{int}	0.0242	0.039	0.027
Refinement			
Refinement on	F^2	F^2	F^2
Data/parameters	1195/94	1255/110	1206/122
R ($F_o>4\sigma(F_o)$), wR	0.0389, 0.109	0.086, 0.131	0.0326, 0.0605
R (all data), wR	0.0433, 0.011	0.013, 0.204	0.050, 0.0639
S	1.067	1.051	1.097
$\Delta\rho_{max}$, $\Delta\rho_{min}$	0.3, −0.2 ($e\,Å^{-3}$)	0.06, −0.07 (nucleons $Å^{-3}$)	0.046, −0.047 (nucleons $Å^{-3}$)

measuring the spectrum of the sample at the lowest temperature of 10 K. The resolution function for the TOF spectrometer can be described by a slightly distorted Gaussian function.

In a second attempt quasielastic scattering was studied using the thermal time-of-flight spectrometer SV29 of Forschungszentrum Juelich. A wavelength of 3.62 Å was selected by first-order reflection from a pyrolytic graphite crystal. The energy resolution in this setup is 0.35 meV (FWHM). The medium flux reactor with 2×10^{14} $n\,cm^{-2}\,s^{-1}$ combined with focusing techniques on the monochromator and large solid angles in the secondary spectrometer yield a high neutron flux on the sample.[35] The shorter wavelength compared to the TOF instrument allows for a somewhat wider energy window.

The inelastic neutron-scattering data were collected at the pulsed fast IBR-2 reactor in Dubna using the inverted geometry time-of-flight spectrometer NERA-PR (Ref. 36) at 20 K. The spectra were converted from neutrons per channel to $S(Q,\omega)$ scattering function per energy transfer. At the energy transfer between 5 and 100 meV the relative INS resolution was estimated to be ca. 3%.

The differential scanning calorimetry (DSC) runs were recorded using a Perkin-Elmer DSC-7 calorimeter in the temperature range of 100–280 K with a scanning rate of 20 K/min.

B. Theoretical methods

The harmonic force field (second derivative of energy with respect to internal coordinates) for isolated molecules of hexamethylbenzene was calculated after geometry optimization using the B3LYP model at the 6-31G (d,p) level as implemented in GAUSSIAN 98 package.[37] The potential-energy distributions (PED) for normal modes were calculated using the GAMESS program[38] on the B3LYP/6-31G(d,p) level.

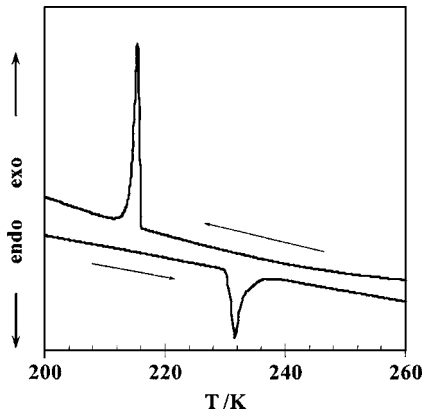

FIG. 1. DSC runs on cooling and heating for HMB·TCNQ complex (DSC ramp rate of 20 K/min; sample mass 11.7 mg).

The corresponding modes were defined by means of internal coordinates according to Pulay *et al.*[39]

Inelastic neutron spectra were reproduced based on calculated mass weighted normal vibrational coordinates using auntieCLIMAX program,[40] which is a modified personal computer (PC) version of the CLIMAX program adapted to parameters of the NERA-PR spectrometer.

III. RESULTS AND DISCUSSION

A. DSC

The results of the calorimetric analysis for HMB·TCNQ complex are illustrated in Fig. 1. When the sample is heated and cooled from 100 up to 280 K it reveals one reversible heat anomaly at 230/218 K (heating-cooling) with the temperature hysteresis—12 K. The existence of temperature hysteresis and well-shaped peaks on the DSC runs may indicate a first-order phase transition. The phase transition is accompanied by a heat effect equal to 1.75 kJ/mol. This value is close to that determined for the high-temperature transition (384 K) in HMB itself.[2]

B. Structural studies

Both x-ray and neutron-diffraction studies confirm a disorder at higher temperatures connected with the rotation of methyl groups, while no rotation of the whole HMB molecules around the sixfold axis was detected. Simultaneously no structural phase transitions in the HMB·TCNQ crystal were revealed.

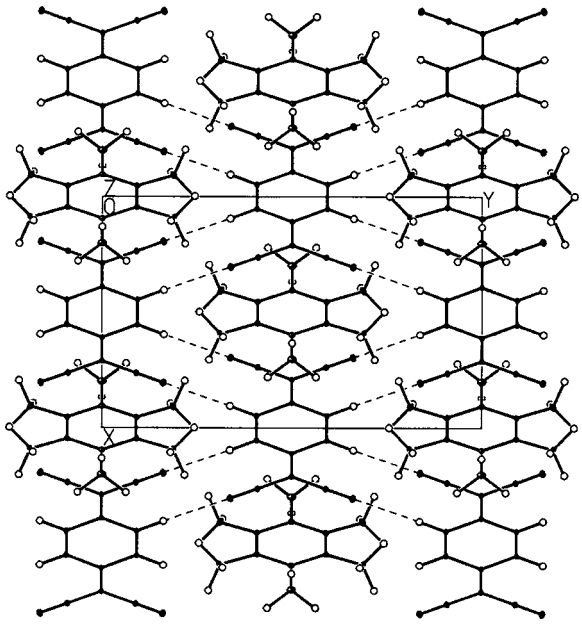

FIG. 3. Packing of molecules in HMB·TCNQ crystal; the view along the *c* axis.

The neutron-diffraction measurements at 100 K enabled unequivocal determination of configuration of HMB·TCNQ complexes. The planes of HMB and TCNQ molecules form a small angle equal to ca. 6° that enables approaching of dicyanomethylene group to the HMB molecule to the distance of 3.34 Å, i.e., characteristic of relatively strong CT π complexes. This configuration is shown in Fig. 2(b). The neutron-diffraction studies at 100 K enabled the conformation of methyl groups to be determined with high accuracy; their orientation changes alternately by going around the axis perpendicular to the HMB molecule plane. The packing of molecules in the lattice is illustrated in Fig. 3.

The main structural parameters of the HMB·TCNQ complex are presented in Table II. The contacts of the C–H bonds with nitrogen atoms are characterized by geometrical parameters given in Table III.

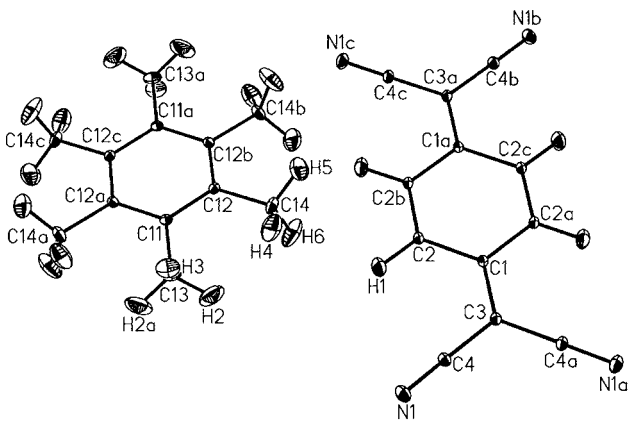

FIG. 2. (a) The structure and numbering scheme of the HMB TCNQ complex. Displacement ellipsoids are shown at the 30% probability level. Symmetry code used to generate equivalent atoms: (i) $x,-y,z$; (ii) $1-x,y,-z$; (iii) $1-x,-y,-z$ for HMB and (i) $x,-y,z$; (ii) $-x,y,-z$; (iii) $-x,-y,-z$ for TCNQ. (b) The molecular overlap as seen perpendicular to the mean molecular planes.

TABLE II. Selected bond length (Å) and angles (°) in HMB TCNQ complex determined at 100 K by neutron diffraction.

Molecule TCNQ	
N(1)–C(4)	1.1564(11)
C(1)–C(3)	1.3800(18)
C(1)–C(2)	1.4458(11)
C(2)–C(2)^{i}	1.3574(18)
C(3)–C(4)	1.4282(11)
C(2)–H(1)	1.085(2)
Molecule HMB	
C(11)–C(12)	1.4082(11)
C(11)–C(13)	1.5143(19)
C(14)–C(12)	1.5078(14)
C(12)–C(12)^{ii}	1.4052(18)
C(13)–H(2)	1.071(3)
C(13)–H(3)	1.068(3)
C(14)–H(4)	1.082(3)
C(14)–H(5)	1.079(3)
C(14)–H(6)	1.076(3)
Molecule TCNQ	
C(3)–C(1)–C(2)	120.68(6)
C(2)^{iii}–C(1)–C(2)	118.61(11)
C(2)^{i}–C(2)–C(1)	120.69(6)
C(1)–C(3)–C(4)	122.30(6)
C(4)–C(3)–C(4)	115.35(11)
N(1)–C(4)–C(3)	178.05(10)
C(2)^{i}–C(2)–H(1)	119.85(12)
C(1)–C(2)–H(1)	119.46(14)
Molecule HMB	
C(12)–C(11)–C(12)^{iii}	120.08(12)
C(12)–C(11)–C(13)	119.96(6)
C(11)–C(13)–H(2)	112.09(18)
C(11)–C(13)–H(3)	112.6(2)
H(2)–C(13)–H(3)	106.8(2)
C(12)–C(14)–H(4)	12.25(17)
C(12)–C(14)–H(5)	111.35(18)
H(4)–C(14)–H(5)	105.1(3)
C(12)–C(14)–H(6)	112.20(17)
H(4)–C(14)–H(6)	107.9(3)
H(5)–C(14)–H(6)	107.7(3)
C(12)^{ii}–C(12)–C(11)	119.94(6)
C(12)^{ii}–C(12)–C(14)	119.89(6)
C(11)–C(12)–C(14)	120.16(9)

Symmetry code: (i) $-x,y,-z$; (ii) $-x+1,y,-z$; (iii) $x,-y,z$

TABLE III. Hydrogen bond geometries (Å, °).

D–H···A	D···A	D–H	H···A	<(DHA)
C(2)–H(1)…N(1)	3.364(2)	1.085(2)	2.983(2)	119.4(1)
C(2)–H(1)…N(1)^{i}	3.528(1)	1.085(2)	2.497(2)	158.3(2)
C(14)–H(4)…N(1)	3.302(2)	1.082(2)	2.760(3)	110.7(2)
C(14)–H(5)…N(1)^{i}	3.826(2)	1.079(2)	2.788(3)	161.5(3)
C(14)–H(6)…N(1)^{ii}	3.563(2)	1.076(2)	2.679(3)	139.1(3)

Symmetry code: (i) $-x+0.5,-y+0.5,-2+0.5$; (ii) $x+0.5,y+05,z+0.5$

TABLE IV. Calculated and experimental frequencies in [cm^{-1}] of HMB and HMB·TCNQ.

Approximate assignments	Calculated[#]	Experimental INS	
	B3LYP/6-31 G**	HMB	HMB·TCNQ
CH_3 tors	71	130	110
CH_3 tors	75	132	112
CH_3 tors	77	136	122
CH_3 tors	97	157	147
CH_3 tors	99	163	150
CH_3 tors	102	166	153
Ring torsion	125	152	123
Ring torsion	129	155	126
Ring torsion	163	199	169
C–CH_3 wagg	198	230	199
C–CH_3 bend	347	348	350
C–CH_3 bend	347	349	354
C–CH_3 wagg	354	362	369
C–CH_3 wagg	355	362	369
C–CH_3 bend	413	406	412
C–CH_3 bend	416	411	416
C–CH_3 bend	456	451	453
Ring def.	458	453	453
Ring def.	458	455	453
C–CH_3 str	555	555	549
C–CH_3 wagg	585	575	574
C–CH_3 wagg	585	575	575
C–CH_3 bend	590	580	580
Ring def.	593	583	583
C–CH_3	745	724	
C–CH_3	809	802	809
C–CH_3	809	802	809

C. INS

The frequencies of modes below 800 cm^{-1}, associated with the CH_3 groups dynamics, measured for the HMB·TCNQ complex and, for comparison, for HMB itself are presented in Table IV. The analysis of the experimental INS spectra was limited to the dynamics of HMB molecules that seems to be justified by the following reasons. As shown in the INS study on HMB,[13] the INS spectrum of HMB (Fig. 4) is dominated by torsional vibration of CH_3 groups' modes. It is characterized by the high intensity peaks in the transfer energy range of 100–200 cm^{-1}. Some of the peaks in the transfer energy range of 200–400 cm^{-1} can be described as overtones and summation tones of CH_3 torsional modes. For the transfer energy above 400 cm^{-1} the INS peaks are very weak and broad, which makes the INS spectrum above 400 cm^{-1} very hard to be interpreted. Very similar situation is observed for the HMB·TCNQ INS spectrum. This spectrum (Fig. 5) is also dominated by the CH_3 group's torsional vibration modes found in the transfer energy range of 100–200 cm^{-1}. Above 200 cm^{-1} the INS peaks are weak as well as broad. In both the INS spectra lattice vibration modes are observed in the transfer energy range up to 100 cm^{-1}. The contribution of hydrogen atoms of TCNQ molecules to the spectrum in the low-frequency region is negligibly small. As shown in literature[41] only the modes at 484 cm^{-1} into which, accordingly to the methodology of Pulay *et al.*,[39] the

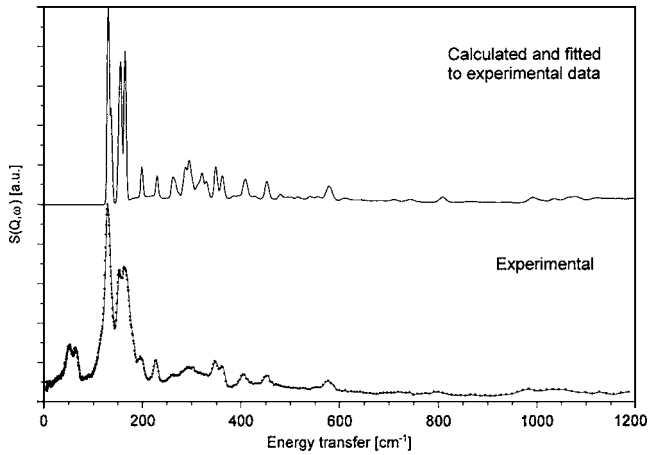

FIG. 4. Experimental (lower) INS spectrum of HMB compared to the theoretical one (after fitting of frequencies).

C–H out-of-plane vibrations contribute in 12%, and at 615 cm^{-1} with 25% contribution of these vibrations could be considered. In addition of substantial importance are the two modes with high contribution of C–H out-of-plane vibrations mainly at 832 cm^{-1} (96%) and 882 cm^{-1} (79%). The other modes with contribution of hydrogen atoms are observed at higher frequencies. Therefore in this paper the frequency region below 800 cm^{-1} is only considered. In assignments of analyzed modes the vibrations which possess the main contribution to a given mode were accepted. The lowest frequencies (six modes) correspond almost 100% to torsional vibrations of CH_3 groups. In modes of higher frequencies the ring torsional vibrations and deformation vibration of the CH_3 groups, of wagging and bending type, show a substantial contribution. In Table IV the calculated frequencies for HMB are compared with the INS experimental ones for both HMB itself and its complex with TCNQ. In Figs. 4 and 5 the experimental spectra are compared with the theoretical ones fitted to experimental to show the correctness of assignments. If one omits the region below 100 cm^{-1} connected with the lattice phonons (into which the TCNQ molecules contribute as well) and limits considerations only to internal modes the agreement seems to be very good and

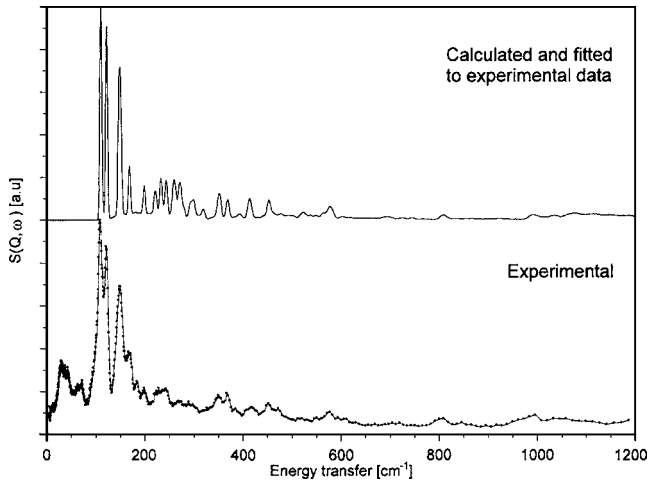

FIG. 5. Experimental (lower) INS spectrum of HMB·TCNQ complex compared to the theoretical one (after fitting of frequencies).

proves the assignments to be correct. The comparison shows, on the other hand, that low-frequency vibrations associated with CH_3 groups, and particularly torsional vibrations below 200 cm^{-1} are characterized by high intensities. Notice that these vibrations are either of very low intensities or not observed at all in the IR and Raman spectra due to the selection rules as has been shown, e.g., in Ref. 42.

The comparison of the calculated (for the gas phase) and experimental frequencies shows that the latter ones are much higher. The difference is the higher the lower is the frequency, i.e., the force constant is lower. These vibrations are particularly sensitive to the interaction in the crystal lattice. One can suggest, according to a rich literature,[43] that these interactions are of type of unconventional hydrogen bonds $C-H\cdots Y$, where Y may be typical proton acceptor atoms such as O and N, but also π electrons.[44] In the crystal lattice of HMB we are dealing with such contacts. As can be seen the packing in the HMB·TCNQ complex is such that molecules are ordered in layers alternately composed of HMB or TCNQ molecules. The stacks are also formed alternately.

It seems surprising that the experimental INS frequencies for the complex are lower than those for neat HMB. However, if one takes into consideration the structure of the solid complex it is understandable that HMB molecules should behave there more freely. Our system can be treated in a way of HMB molecules put into a TCNQ matrix. Certainly the interactions between the methyl groups and the atoms of TCNQ molecules do exist but they are weaker between the layers where the conditions for formation of unconventional hydrogen bonds are less favorable. Notice that except of the first six modes (CH_3 torsion) the calculated and experimental frequencies are in excellent agreement if one takes into account that INS frequencies are burdened by an error exceeding 3%. This result, indicating that CH_3 groups in the complex are more free than in the neat HMB, is in agreement with the QENS results which will be discussed later.

D. QENS

The QENS spectra measured with TOF spectrometer for temperatures from 10 to 290 K are presented in Fig. 6. The spectra measured at 10 and 50 K do not exhibit quasielastic component. The quasielastic broadening begins at 100 K and increases with increasing temperature.

The TOF QENS spectra can be reasonably well described by instantaneous 120° jumps of the CH_3 groups around the threefold symmetry axis with scattering function given by the equation[45,46]

$$S(Q,\omega)=\frac{1}{3}\left(1+\frac{2\sin(Q\cdot r\sqrt{3})}{Q\cdot r\sqrt{3}}\right)\delta(\omega)+\frac{2}{3\pi}\left(1-\frac{\sin(Q\cdot r\sqrt{3})}{Q\cdot r\sqrt{3}}\right)\frac{\Gamma}{\Gamma^2+\omega^2},$$

where Q and ω are the momentum and energy transfers, $r=1.06\ \mathring{A}$ is the distance of the protons from the reorientation axis, $\Gamma=3\hbar/2\tau$, and τ is the mean time between jumps.

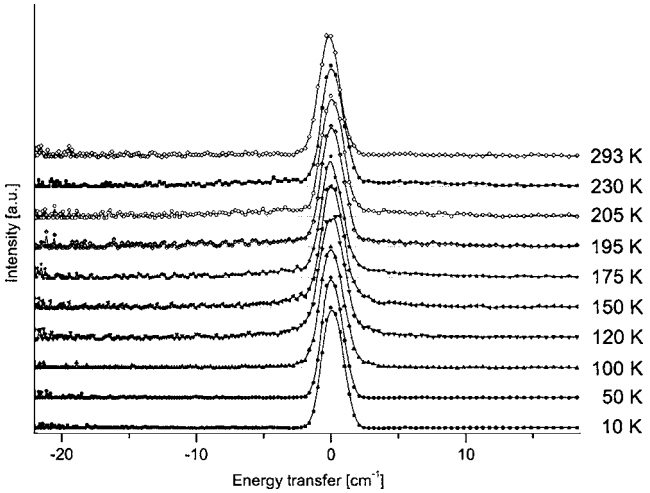

FIG. 6. QENS spectra measured for the temperature range of 10–293 K of HMB·TCNQ complex.

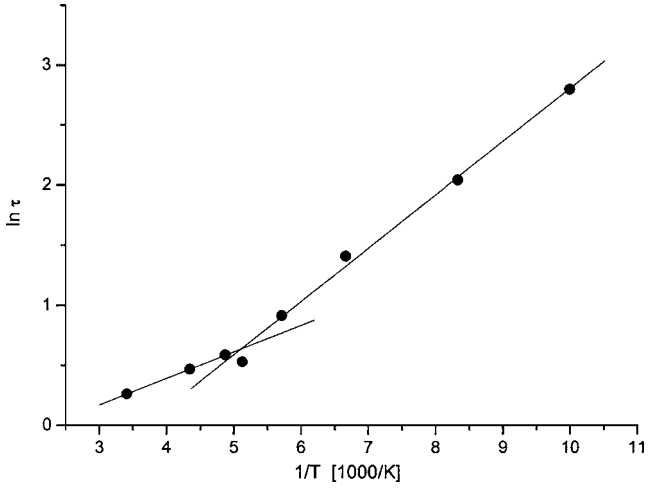

FIG. 8. Temperature dependence of the best-fit mean time between 120° jumps τ. The lines correspond to the Arrhenius formula.

Only the protons from the CH_3 groups of HMB molecules take part in the fast reorientation described by scattering function given above. It is assumed that the protons of TCNQ molecules contribute only to the elastic part of the spectra. The typical results of fitting of the model to the QENS spectra are shown in Fig. 7. The fitted mean time between jumps, τ, changes from 16 ps at 100 K to 1 ps at room temperature. The statistics of the spectra did not allow fits with more than one quasielatic Lorentzian.

The temperature dependence of the best-fit mean time between 120° jumps of the CH_3 groups around threefold symmetry axis is shown in Fig. 8. The data can be described by the Arrhenius formula with different activation barriers in both phases. The fitted activation energy is 3.7 kJ/mol in the low-temperature phase and 1.8 kJ/mol in the high-temperature one. In comparison with the value of 6 kJ/mol obtained for HMB itself[13] the activation energies in HMB·TCNQ crystal are lower. The conclusion can be drawn that methyl groups of HMB molecules in the TCNQ matrix can reorient more freely.

With increasing temperature the elastic part of QENS spectra becomes bigger than predicted by the 120° jumps model. The possible explanation is the fact that the time τ becomes too small for the experimental resolution of the spectrometer and the wings of the QENS part are hidden in the background for the highest temperatures. Also, one cannot exclude the possibility that the character of the reorientation changes. For instance, we cannot exclude the reorientation around the sixfold axis perpendicular to the molecule plane, although the diffraction studies did not confirm such a possibility.

In the case of SV29 spectrometer the sample was measured in the temperature regime from 3 K to room temperature. The results are illustrated in Fig. 9. It focuses on the quasielastic regime and the low-temperature regime.

The spectra taken at 3, 60, 100, 130, and 160 K are shown. At 100 K a wing of the resolution function shows that the quasielatic scattering enters the energy window of the spectrometer. Already at 60 K a soft inelastic mode at ~3 meV shows up. This mode increases in intensity and softens. At 160 K its energy is close to 2.5 meV. It now overlaps with the quasielastic intensity and makes a fitting impossible. All parameters strongly depend on the modeling of the inelastic mode. Furthermore the Bragg reflections contaminate the elastic intensity. Thus we cannot force a fit to obey the ratio of elastic and quasielastic scattering deduced from the scattering function for 120° jumps of the methyl

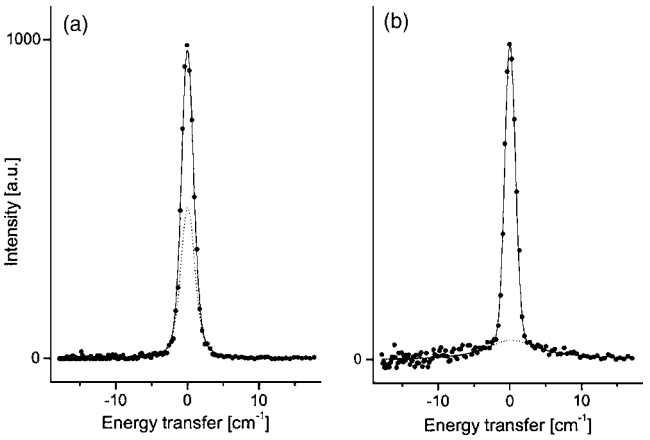

FIG. 7. Example of fitting the 120° jumps model to the QENS spectra for 100 K (a) and 195 K (b) of HMB·TCNQ complex. The broken line represents the quasielastic component.

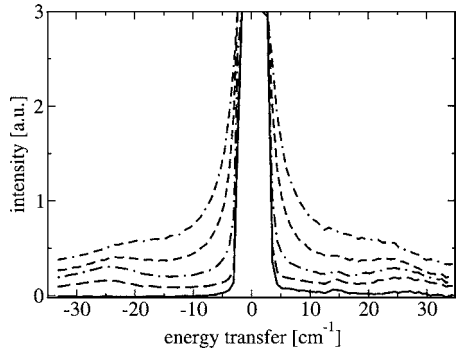

FIG. 9. Evolution of the low-energy regime of HMB·TCNQ with increasing the temperature. Temperatures are (from bottom) 3, 60, 100, 130, and 160 K.

groups. These are the reasons why quasielastic studies generally use cold neutron time-of-flight spectrometers.

The new feature in the SV29 spectra is the soft inelastic mode. Lattice dynamical calculations would be needed to identify its character. Without such calculations we may suggest a pure mass effect. For comparison we consider a simple heavy alkali atom, cesium, with $m=133m_p$, m_p being the mass of a proton. The zone boundary phonon energies are about 5 meV. The heavier masses of HMB and TCNQ with $162m_p$ and $192m_p$, respectively, lead to softer zone boundary acoustic modes where neighboring molecules move in antiphase.

Under the assumption of a purely threefold rotational potential the activation energy of 3.1 kJ/mol is connected with a rotational barrier height $V_3=39$ meV. The methyl librational energy in this potential is 13.5 meV. This value fits very nicely to the strong band observed in the weighted vibrational density of states (VDOS) as assigned in Table IV. In the single-particle model of methyl group rotation the librational ground state should then be split by 3.6 μeV, which is not observed. A moderate change of the shape of the rotational potential by a higher-order Fourier term V_6 cannot explain the discrepancy. A possible solution may be based on the structure of the HMB molecule. The six methyl groups on the benzene rings may not be free but interact with each other. Rotational tunneling of coupled methyl groups has been treated theoretically.[47] The main result with respect to our problem is that the tunneling splitting is reduced with the number of interacting methyl groups while the other modes, librations and activation energy, stay almost unchanged. Another proof of coupling may be seen in the large number of librational modes (Table IV), which in a single molecule model likely represent eigenmodes of the six coupled methyl groups.

IV. CONCLUSIONS

The condition, in which the HMB molecules in the HMB·TCNQ crystal exist, can be treated as in a matrix formed by the sublattice of TCNQ molecules. The disorder at higher temperatures is connected with the rotation of methyl groups. There is no evidence of the rotation of the whole molecules around the sixfold symmetry axis. The charge-transfer interaction between the alternately located HMB and TCNQ molecules in columns along the *a* axis is so strong that it leads to the fixation of mutual orientation of HMB and TCNQ molecules. On the other hand, the planar ordering causes some decrease of the barrier to the CH_3 groups rotation. This is reflected in the results of QENS when comparing the temperature dependence of the quasielastic scattering function for the neat HMB and its complex. Simultaneously in the INS spectra in the low-frequency region related to the modes ascribed to the CH_3 torsional vibrations, the frequencies in complexes are lower than those in neat HMB. This can be interpreted as weakening of the interaction with the environment.

Here we want to emphasize the role of unconventional (blueshifting) C–H···Y hydrogen bonds in such interactions. It seems that the INS technique is particularly useful in studies of unconventional hydrogen bonds in the solid state. The torsional vibrations of CH_3 groups are characterized by particularly high intensity in the INS spectra while these modes in conventional spectroscopic IR and R methods are either not visible at all (selection rules) or are characterized by very low intensity.

The decrease of the frequency of torsional modes of CH_3 groups is understandable when analyzing the structures of HMB and HMB·TCNQ. In the case of neat HMB the CH_3 groups are engaged in formation of C–H···π bridges. On the other hand, the parallel arrangement of HMB and TCNQ molecules in the crystalline complex does not correspond to the favorable orientation towards both π and *n* electrons of the cyano nitrogen atoms. The main packing forces are due to the charge-transfer π-π interaction.

ACKNOWLEDGMENTS

This work has been supported partially by the Polish Ministry of Science and Informatics (Grant No. 4 T09A 05125) and by the European Community-Access to Research Infrastructure action of the Improving Human Potential Program; Contract No. HPRI-CT 1999-00061.

[1] J. M. Adams, A. S. Ivanov, M. R. Johnson, and J. A. Stride, Physica B **350**, 351 (2004).
[2] NIST Chemistry Web Book: www.nist.gov.
[3] G. Celotti *et al.*, Acta Crystallogr. **A31**, 582 (1975).
[4] P. Le Magueres *et al.*, Organometallics **20**, 115 (2001).
[5] W. C. Hamilton and J. W. Edmonds, American Crystallographic Association, Abstract Papers 18 (1971).
[6] K. Izumi, J. Cryst. Growth **169**, 325 (1996).
[7] Y. Shen, T. Wu, and Y. Yang, Chem. Phys. Lett. **242**, 83 (1995).
[8] J. Taug, L. Sterna, and A. Pines, J. Magn. Reson. **41**, 389 (1980).
[9] E. Rössler, M. Taupitz, K. Börner, M. Schulz, and H. -M. Vieth, J. Chem. Phys. **92**, 5847 (1990).
[10] K. Börner, G. Diezemann, E. Rössler, and H. -M. Vieth, Chem. Phys. Lett. **181**, 563 (1991).
[11] B. Jansen-Glaw, E. Rössler, M. Taupitz, and H. -M. Vieth, J. Chem. Phys. **90**, 6858 (1989); **115**, 3241 (2001).
[12] G. L. Hoatson, R. L. Vold, and T. Y. Tse, J. Chem. Phys. **100**, 4756 (1994).
[13] J. Krawczyk, J. Mayer, I. Natkaniec, M. Nowina-Konopka, A. Pawlukojć, O. Steinsvoll, and J. A. Janik, Physica B **362**, 271 (2005).
[14] N. D. Jones and R. E. Marsh, Acta Crystallogr. **15**, 809 (1962).
[15] M. Saheki, H. Yamada, H. Yoshioka, and K. Nakatsu, Acta Crystallogr. **B32**, 662 (1976).
[16] D. Britton, Acta Crystallogr. **C44**, 2222 (1988).
[17] T. Dahl, Acta Chem. Scand. (1947-1973) **26**, 1569 (1972).
[18] H. Bock, M. Sievert, H. Schodel, and M. Kleine, Z. Naturforsch., B: Chem. Sci. **51**, 1521 (1996).
[19] D. S. Reddy, B. S. Goud, K. Panneerselvam, and G. R. Desiraju, Chem. Commun. (Cambridge) 1993, 663.
[20] T. Dahl, Acta Chem. Scand. **44**, 56 (1990).
[21] P. Le Magueres, S. V. Lindeman, and J. K. Kochi, J. Chem. Soc., Perkin Trans. 2 **2**, 1180 (2001).
[22] R. H. Colton and D. E. Henn, J. Chem Soc. B **0**, 1532 (1970).
[23] C. K. Johnson, H. L. Reed II, R. F. Hall, and V. F. Raaen, American Crystallographic Association, Abstract Papers 135 (1974).
[24] T. Kundu, B. Pradhan, and B. S. Singh, Proc.-Indian Acad. Sci., Chem. Sci. **114**, 623 (2002).
[25] A. J. Horsewill, Spectrochim. Acta, Part A **48**, 379 (1992).
[26] M. Prager and A. Heidemann, Chem. Rev. (Washington, D.C.) **97**, 2933 (1997).
[27] M. R. Johnson and G. J. Kearley, Annu. Rev. Phys. Chem. **51**, 297 (2000).
[28] A. Pawlukojć and L. Sobczyk, Trends Appl. Spectr. **5**, 117 (2004).
[29] G. M. Sheldrick, Acta Crystallogr. **A46**, 467 (1990).

[30] G. M. Sheldrick, SHELXL 97, Program for the Refinement of Crystal Structures, University of Göttingen, Germany (1997).
[31] M. S. Lehman and F. K. Larsen, Acta Crystallogr. **A30**, 580 (1974).
[32] P. Coppens, L. Leiserowitz, and D. Rabinovich, Acta Crystallogr. **18**, 1035 (1965).
[33] V. F. Sears, Neutron News **3**, 26 (1992).
[34] J. O. Landgren, Crystallographic Computer Program, Report UUIC-B13-4.05. Institute of Chemistry, University of Uppsala, Sweden, 1982.
[35] M. Prager, Physica B **283**, 376 (2000).
[36] I. Natkaniec, S. I. Bragin, I. Brankowski, and J. Mayer, *Proceedings of ICANS-XIII*, Abington, 1993 [RAL Report No. 94-025 (unpublished)], Vol. 1, p. 89.
[37] M. J. Frisch *et al.*, Gaussian 98, Rev. A.9 programme, Gaussian. Inc., Pittsburgh PA, 1998.
[38] M. W. Schmidt, K. K. Baldrige, J. A. Boatz *et al.*, J. Comput. Chem. **14**, 1347 (1993).
[39] P. Pulay, G. Fergasi, F. Pang, and J. E. Boggs, J. Am. Chem. Soc. **101**, 2550 (1979).
[40] J. Tomkinson, A. J. Ranirez-Cuesta, W. Champion, J. W. Lawrence, and S. F. Parkers, auntieCLIMAX, a users guide.
[41] A. Pawlukojć, I. Natkaniec, G. Bator, L. S. Obczyk, and E. Grech, Chem. Phys. Lett. **378**, 665 (2003).
[42] A. Pawlukojć, I. Natkaniec, G. Bator, L. Sobczyk, E. Grech, and J. Nowicka-Scheibe, Spectrochim. Acta (in press).
[43] G. R. Desiraju and T. Steiner, *The Weak Hydrogen Bond in Structural Chemistry and Biology* (Oxford University Press, New York, 1999).
[44] S. Scheiner and S. J. Grabowski, J. Mol. Struct. **615**, 203 (2002).
[45] T. Springer, *Springer Tracts in Modern Physics* (Springer, Berlin, 1972), Vol. 64.
[46] J. D. Barnes, J. Chem. Phys. **58**, 5193 (1973).
[47] M. Timan, G. Voll, and W. Haeusler, J. Chem. Phys. **100**, 8307 (1994).